ICARUS 100, 187–196 (1992)

Submillimeter Continuum Emission from Comets

DAVID JEWITT[1]

Institute for Astronomy, University of Hawaii, 2680 Woodlawn Drive, Honolulu, Hawaii 96822

AND

JANE LUU[1,2]

Center for Astrophysics, Harvard University, 60 Garden Street, Cambridge, Massachusetts 02138

Received June 1, 1992; revised August 10, 1992

We report submillimeter continuum observations of five comets obtained at the James Clerk Maxwell Telescope on Mauna Kea. Two of the five comets (P/Brorsen–Metcalf and Okazaki–Levy–Rudenko) were detected at 800-μm wavelength, while physically significant upper limits were placed on the other three (Austin 1989c$_1$, P/Faye, and Levy 1990c). We compare the JCMT data with millimeter continuum measurements of Comets Austin 1989c$_1$, IRAS–Araki–Alcock, and P/Halley from the published literature. The submillimeter and millimeter signals are tentatively ascribed to thermal emission from porous particles in the coma, with total particle masses $M \sim 10^7$–10^8 kg. Previous explanations in terms of ice grain halos and near-nucleus boulder-clouds are less plausible, as they require inordinately large particle masses.

1. INTRODUCTION

The cometary nucleus is a kilometer-sized body consisting of an intimate mixture of refractory matter and frozen volatiles. The dominant cometary volatile is water ice (Whipple 1950). At heliocentric distances $R \leq 5$ AU, heating by the Sun causes the water ice to sublimate and expand into the vacuum of interplanetary space. Drag forces expel embedded dust into the cometary coma, where it may be observed using a variety of ground based techniques. Cometary dust gives rise to a continuum of scattered radiation at visible and near-infrared wavelengths ($0.3 \leq \lambda \leq 5$ μm) and a continuum of thermal emission in the infrared.

It has long been realized that the thermal continuum must extend to radio wavelengths, and that study of the radio continuum emission might constrain important properties of the cometary dust. For instance, long wavelength radiation can be efficiently radiated from large particles and so might provide a useful probe of these particles. The existence of large particles in comets is known from four independent measurements. First, visible meteors consist of 0.1- to 1-mm-sized debris from active comets (Williams 1990). Second, radar observations of Comets IRAS–Araki–Alcock (Goldstein *et al.* 1984, Harmon *et al.* 1989) and P/Halley (Campbell *et al.* 1989) have revealed backscatter from large near-nucleus grains. Third, thermal maps from IRAS have revealed dust trails in the orbits of many comets (Davies *et al.* 1984, Eaton *et al.* 1984, Sykes *et al.* 1986). The narrowness of these trails suggests large particles with characteristic sizes in the millimeter range. Fourth, large particles were detected in the coma of Comet P/Halley by impact counters on the Giotto spacecraft (McDonnell *et al.* 1987). Indeed, the premature termination of the Giotto encounter is attributed to a collision between the spacecraft and a millimeter-sized grain within 10^3 km of the nucleus (Reinhard 1987).

There is a long history of attempted observations of the cometary radio continuum (see reviews by Gibson and Hobbs (1981), Snyder (1982), and Crovisier and Schloerb (1991) for brief histories of this subject). A majority of the early observations were made at wavelengths $\lambda > 1$ cm, where the thermal continuum is expected to be very weak, and some of the observations utilized inaccurate ephemerides (c.f. Snyder 1982). Partly for these reasons, most of the early observations yielded only upper limits to the strength of the radio continuum. In a few cases, large but transient signals were reported, namely in Kohoutek (1973f) at λ = 28 and 37 mm (Hobbs *et al.* 1975) and in Comet West at λ = 37 mm (Hobbs *et al.* 1977). An icy

[1] Visiting astronomer at the James Clerk Maxwell Telescope, operated by the Royal Observatory Edinburgh on behalf of the Science and Engineering Research Council of the United Kingdom, the Netherlands Organisation for Scientific Research, and the National Research Council of Canada.

[2] Present address: Department of Astronomy, 601 Campbell Hall, U.C. Berkeley, Berkeley, CA 94720.

0019-1035/92 $5.00

grain halo model was advanced to account for the transient emission (Hobbs *et al.* 1975, Gibson and Hobbs 1981). However, the model invoked an optically thick halo of centimeter-sized grains that is difficult to reconcile with our present understanding of comets.

The purpose of the present paper is to describe an initial submillimeter survey of five near-Earth comets made using the James Clerk Maxwell Telescope (JCMT) on Mauna Kea. The new observations are distinguished from the above-mentioned efforts in two respects. First, we observed at both submillimeter and millimeter (as opposed to centimeter) wavelengths. Thermal emission from dust is expected to have flux density $S_\nu \sim \lambda^{-\alpha}$, where λ is the wavelength and $\alpha \geq 2$ ($\alpha = 2$ corresponds to the Rayleigh–Jeans blackbody spectrum). Thus, the use of shorter wavelengths gives us a strong advantage for the detection of a thermal continuum. Second, we have obtained simultaneous astrometry from optical telescopes to verify the cometary ephemerides used at the JCMT. Thus, our observations are not susceptible to the ephemeris uncertainties which plagued some of the earlier observations (Snyder 1982).

The first result of our survey, the detection of Comet P/Brorsen–Metcalf at 800 μm, has been separately published (Jewitt and Luu 1990, hereafter JL90). In Section 2, we describe pertinent details of the submillimeter observations. In Section 3, we present results from all five comets observed with the JCMT. Finally, in Section 4, we interpret the JCMT observations and compare them with independent millimeter observations by Altenhoff and collaborators (Altenhoff *et al.* 1983, 1986, 1989).

2. OBSERVATIONS

The present observations were taken using the James Clerk Maxwell Telescope (JCMT) located on Mauna Kea, Hawaii. This 15-m-diameter telescope is diffraction-limited at wavelengths $0.35 \leq \lambda \leq 1.3$ mm. A significant characteristic of the JCMT is its remarkable mechanical stability. The telescope can point to an accuracy ±2–3 arcsec over the whole sky, while offsets from nearby objects of known position are accurate generally to about ±1 arcsec. Observations are made through a plastic membrane which acts both as a windshield and as a sunscreen. The membrane permits observations of near-Sun comets to be made while minimizing the deleterious effects of solar heating of the telescope. These advantages substantially outweigh a ~10% loss in sensitivity due to extinction in the membrane.

All observations described below were taken using a single channel, He^3-cooled bolometer, UKT14 (Duncan *et al.* 1990). In general, we used a 65-mm-diameter circular aperture for observations at $\lambda = 0.8$ mm. This corresponds to 18 arcsec diameter in the plane of the sky, slightly larger than the 14 arcsec diffraction limit at this wavelength. The entrance aperture of UKT14 is chopped at 7.8 Hz to permit sky subtraction. The chop amplitude was either 40 or 60 arcsec in azimuth, depending on atmospheric conditions. In addition, the telescope is periodically nodded along the chopping direction to guard against possible asymmetries between the sensitivities of the on-source and chopped beams. Numerous observations of blank fields confirmed the success of the chopping and nodding algorithms; such observations always gave net signals consistent with zero. Observing efficiency (time integrating on-source/total elapsed time) is reduced by the need to observe object and sky positions for equal times. It is further reduced by mechanical and software overheads in the chop and nod algorithms. The observing efficiency was found to be ~30% for the present observations.

The maximum sensitivity of the JCMT when used to observe a Rayleigh–Jeans spectrum (flux density $S_\nu \propto \lambda^{-2}$) occurs near $\lambda = 0.8$ mm. At shorter wavelengths, atmospheric extinction and sky noise reduce the sensitivity, while at longer wavelengths the spectrum is intrinsically fainter, and the focal plane image is imperfectly matched to the bolometer entrance aperture. Therefore, a majority of the present observations were taken using a broadband filter of effective wavelength $\lambda = 0.8$ mm and fractional width $\Delta\lambda/\lambda \sim 0.25$ (Duncan *et al.* 1990).

Cometary ephemerides were generally obtained using a program provided by David Tholen of the Institute for Astronomy, based on orbital elements computed by Brian Marsden of the Center for Astrophysics. The ephemeris positions were refined in real time using optical observations from the University of Hawaii 2.2-m telescope or from the NASA Infrared Telescope Facility. Positional errors of the comets were frequently found to be larger than the JCMT beam, so that the optical correction of the ephemerides was vital to the success of these observations.

Tracking of the JCMT at cometary rates was achieved using a program to linearly interpolate the right ascension and declination between given starting and ending positions. The interpolation interval was kept at less than 3 hr; this was small enough to guarantee the validity of the linear interpolation to better than 1 arcsec. The interpolation algorithm was tested repeatedly using bright asteroids.

The accuracy of submillimeter photometry is limited by the properties of the terrestrial atmosphere. The high altitude of Mauna Kea leads to exceptionally good submillimeter observing conditions, when compared to conditions at lower sites. Three atmospheric effects are important at submillimeter wavelengths. First, atmospheric attenuation or "extinction" is produced primarily by water vapor above the telescope. On a good night, the quantity of precipitable water above the JCMT is ≤1 mm, and the resulting extinction at $\lambda = 0.8$ mm is of order 10% per airmass. The submillimeter extinction is rarely spatially uniform, however, and pronounced variations in extinction are seen both with respect to azimuth at constant elevation and with respect to time. These spatial and temporal variations are removed at the telescope by means of frequently repeated observations of flux reference sources at small angular distance from the target comet. Second, the brightness of the submillimeter sky fluctuates rapidly in response to atmospheric inhomogeneities in the telescope beam. These fluctuations give rise to "sky noise" over and above the noise expected from counting statistics alone. Third, "anomalous refraction" is an angular excursion of the image produced by refraction through parcels of moist air above the telescope. Its observational signature is enhanced nonrandom noise in the bolometer signal, due to the movement of the image in and out of the photometry beam. As all three effects decrease in severity with increasing wavelength, we took data at 1.1 mm instead of 0.8 mm on poor nights.

TABLE I
Photometry of Okazaki–Levy–Rudenko

Comet[a]	UT date[b]	R [AU][c]	Δ [AU][d]	α [deg][e]	λ [mm][f]	S_ν [mJy][g]
O–L–R	1989/Nov/18	0.655	0.661	97.3	0.8	39 ± 12
	1989/Nov/19	0.660	0.642	98.7	0.8	37 ± 20
	1989/Nov/20	0.665	0.624	100.0	0.8	71 ± 20
	1989/Nov/22	0.678	0.591	102.0	0.8	115 ± 42
	1989/Nov/23	0.685	0.576	102.8	0.8	11 ± 7
	1989/Nov/24	0.692	0.563	103.3	0.8	9 ± 7
	Mean	0.673	0.610	100.7	0.8	21 ± 4

[a] Comet name.
[b] UT date of observation.
[c] Heliocentric distance [AU].
[d] Geocentric distance [AU].
[e] Phase angle [degrees].
[f] Wavelength of observation [mm].
[g] Measured flux density [mJy].

3. RESULTS

Comet Okazaki–Levy–Rudenko (1989r)

Comet Okazaki–Levy–Rudenko was observed UT 1989 November 18–20 and 22–24. The primary pointing and calibration source was Mars, for which we adopted the 0.8-mm flux density $S_{0.8} = 222$ Jy (brightness temperature $T_B = 210$ K) on each night. The positional offset of O–L–R relative to the ephemeris position was determined on UT November 18, 19, and 20 using the TV guider camera on the NASA-IRTF, and JCMT observations on these nights were based on the IRTF positions. Subsequent observations were made according to a revised ephemeris incorporating the IRTF astrometry, kindly provided by B. Marsden.

Comet O–L–R was found to be a weak but persistent source at 800 μm (Table I). Note that the nightly means are all positive, although 3σ detections are not achieved on all nights. The weighted mean flux density from all six nights is 21 ± 4 mJy (a 5σ detection). The reported visual magnitude of the comet was $V \sim 6$ (IAUC 4908).

Comet P/Brorsen-Metcalf (1989o)

Our observations of this comet have been presented in full in JL90. Here we summarize the observations for comparison with the other comets (see Table II). The visual magnitude was $V \sim 6$ (IAUC 4851).

Comet Austin (1989c1)

Observations were obtained UT 1990 April 25 and 26 at 800 μm. The primary pointing and flux calibration sources were Mars ($S_{0.8} = 619$ Jy; $T_B = 222$ K) and Uranus ($S_{0.8} = 85$ Jy; $T_B = 84$ K), while CRL 2688 was used as an intermediate standard (Sandell 1992). Astrometric positions accurate to ±2 arcsec were obtained simultaneously at the NASA-IRTF and passed to the JCMT by telephone. Comet Austin was not detected on either night of observation at 800 μm. The combined 3σ flux-density limit is $S_{0.8} < 37.5$ mJy (Table II). The visual magnitude of the comet was $V \sim 5$ (IAUC 4999, 5004).

Comet Levy (1990c)

Observations were obtained UT 1990 August 2 and 3. The primary pointing and calibration source was Mars, for which $S_{0.8} = 1311$ Jy ($T_B = 221$ K) and $S_{1.1} = 697$ Jy ($T_B = 220$ K). Corrections to the best available ephemeris were made based on simultaneous astrometry from the NASA-IRTF on both nights of observation.

Within the uncertainties of observation, Comet Levy was not detected at the JCMT. The 3σ limit to the flux density obtained by combining data from both nights is $S_{1.1} < 13.5$ mJy (Table II). The visual magnitude of the comet was $V \sim 6$ (IAUC 5070).

Comet P/Faye (1948h)

Comet P/Faye was observed UT 1991 November 19 and 20. The primary pointing and calibration source was Uranus, for which we used $S_{0.8} = 73.5$ Jy ($T_B = 84$ K) and $S_{1.1} = 43.4$ Jy ($T_B = 93$ K). Neptune was also observed, with adopted flux densities $S_{0.8} = 27.5$ Jy ($T_B = 79$ K) and $S_{1.1} = 16.6$ Jy ($T_B = 88$ K). Corrections to the best available ephemeris were made based on simultaneous astrometry from the University of Hawaii 2.2-m telescope on both nights of observation.

Within the uncertainties of observation, Comet Faye was not detected at the JCMT. The 3σ limit to the flux density obtained by combining data from both nights is

TABLE II
Other JCMT Photometry

Comet	UT date	R [AU]	Δ [AU]	α [deg]	λ [mm]	S_ν [mJy]
P/Brorsen-Metcalf	1989/Sep/08	0.49	1.05	71.5	0.8	≤24
	1989/Sep/09	0.48	1.07	69.1	0.8	≤40
	1989/Sep/10	0.48	1.10	66.7	0.45	≤515
	1989/Sep/10	0.48	1.10	66.7	0.8	90 ± 18
	1989/Sep/10	0.48	1.10	66.7	1.1	45 ± 13
Austin 1989c_1	1990/Apr/25	0.56	0.66	110.3	0.8	2.7 ± 21.8
	1990/Apr/26	0.58	0.64	110.5	0.8	0.2 ± 15.2
	Mean	0.57	0.65	110.4	0.8	1.0 ± 12.5
Levy 1990c	1990/Aug/02	1.68	0.91	31.3	1.1	3.1 ± 6.8
	1990/Aug/03	1.67	0.88	31.0	1.1	3.4 ± 6.1
	Mean	1.67	0.90	31.2	1.1	3.3 ± 4.5
P/Faye	1991/Nov/19	1.59	0.66	18.1	1.1	4.0 ± 3.4
	1991/Nov/20	1.59	0.66	18.6	1.1	7.8 ± 3.6
	Mean	1.59	0.66	18.4	1.1	5.8 ± 2.5

$S_{1.1} < 7.5$ mJy (Table II). The visual magnitude of the comet was $V \sim 9.5$ (IAUC 5382, 5407).

4. DISCUSSION

In addition to the JCMT observations summarized in Tables I and II, we collect other millimeter wavelength continuum observations in Table III. These include detections of P/Halley at two heliocentric distances and wavelengths by Altenhoff *et al.* (1986, 1989) and of the near-Earth comet, IRAS–Araki–Alcock (Altenhoff *et al.* 1983). We did not include submillimeter observations of the large, distant comet 2060 Chiron (Jewitt and Luu 1992), since this object has unusual physical properties which distinguish it from the other comets in this paper.

In principle, thermal emission might be detected from cometary plasma, from the cometary nucleus, or from dust particles in the coma. We consider these sources separately.

4.1. Plasma

Cometary plasma is generated by photoionization of neutral molecules sublimated from the nucleus. The plasma emits continuum radiation as a result of free–free transitions. The free–free emission coefficent j_ν (W m^{-3} sr^{-1} Hz^{-1}) is (Spitzer 1978)

$$j_\nu = 5.44 \times 10^{-52} \frac{g_{\rm ff} Z_{\rm i}^2 N_{\rm e} N_{\rm i}}{T_{\rm e}^{1/2}} \exp\left\{\frac{-h\nu}{kT_{\rm e}}\right\}, \quad (1)$$

where $g_{\rm ff} \sim 1$ is the Gaunt factor for free–free transitions, $Z_{\rm i}$ is the charge of the ions in units of electrons, $N_{\rm e}$ (m^{-3}) is the electron density, $N_{\rm i}$ (m^{-3}) the ion density, $T_{\rm e}$ (K) the electron temperature, and the other symbols are as previously defined. In the submillimeter region, $h\nu \ll kT_{\rm e}$, so that the exponential in Eq. (1) is close to unity. The predominant source of electrons in the inner coma is H_3O^+ (Balsiger *et al.* 1986). Inside the contact surface of

TABLE III
Other Photometry

Comet	UT date	R [AU]	Δ [AU]	α [deg]	λ [mm]	S_ν [mJy]	Reference
IRAS–Araki–Alcock	1983/May/11	1.00	0.031	105	13.0	9.0 ± 0.7	Altenhoff *et al.* (1983)
P/Halley	1985/Nov–Dec	1.60	0.63	9	3.5	5.9 ± 1.4	Altenhoff *et al.* (1986)
	1985/Nov–Dec	1.60	0.63	9	1.3	52 ± 15	Altenhoff *et al.* (1986)
	1986/Mar	1.13	0.59	62	1.2	52 ± 5	Altenhoff *et al.* (1989)
Austin 1989c_1	1990/Mar/16	0.74	1.46	38	1.2	13 ± 3	Altenhoff *et al.* (1990)

radius r_0, the H_3O^+ number density varies with radial distance from the nucleus approximately as $N_i = N_e = N_0 (r_0/r)$, where N_0 and r_0 are constants (Schwenn *et al.* 1987). The volume integral $S_\nu^{ff} = \int_0^{r_0} 4\pi j_\nu r^2/\Delta^2 \, dr$ gives the free–free flux density

$$S_\nu^{ff} = 6.84 \times 10^{-51} \frac{g_{ff} Z_i^2 N_0^2 r_0^3}{T_e^{1/2} \Delta^2} \quad (2)$$

with units [W m^{-2} Hz^{-1}]. In Eq. (2), Δ (m) is the geocentric distance, and the electron density is taken to be zero at distances $r > r_0$.

We consider Comet P/Halley for reference, since this is the comet in which the plasma parameters are best known. In P/Halley, $N_0 = 10^9$ m^{-3} at $r_0 = 4 \times 10^7$ m, $T_e \sim 10^3$ K, $Z_i = 1$ (Schwenn *et al.* 1987). We find by substitution in Eq. (2) that a Halley-like comet at $\Delta = 1$ AU would give $S_\nu^{ff} \sim 6 \times 10^{-34}$ W m^{-2} Hz^{-1} (6×10^{-5} mJy). This is far smaller than the flux densities listed in Tables I–III and far smaller than can be detected using current technology. Even allowing that we have underrepresented the geometric complexities of the cometary plasma (Balsiger *et al.* 1986, Schwenn *et al.* 1987), it seems safe to conclude that free–free continuum contributes negligibly to the submillimeter and millimeter spectrum.

4.2. Nucleus

The submillimeter emission from the nucleus can be estimated under the assumption of thermal equilibrium. In this case, the flux density S_ν (W m^{-2} Hz^{-1}) at wavelength λ [m] produced by a spherical nucleus of diameter d (m) is given by (Jewitt and Luu 1992)

$$S_\nu = \frac{k\,\varepsilon_{sm}\,\pi\,d^2}{2\,\lambda^2\,\Delta^2} \left(\frac{F_{Sun}}{\sigma R^2}\right)^{1/4} \left(\frac{1-A}{\varepsilon_{ir}\,\chi}\right)^{1/4}, \quad (3)$$

where $k = 1.38 \times 10^{-23}$ J K^{-1} is Boltzmann's constant, $\sigma = 5.67 \times 10^{-8}$ W m^{-2} K^{-4} is Stefan's constant, $F_{Sun} = 1360$ W m^{-2} is the solar constant, ε_{sm} and ε_{ir} are the emissivities at the submillimeter wavelength of observation and at the Planck maximum in the infrared, respectively, A is the Bond albedo, $2 \le \chi \le 4$ is a parameter that depends on the surface distribution of temperature on the nucleus. The heliocentric distance of the nucleus is R [AU].

The emission from a spherical, isothermal blackbody can be computed from Eq. (3) by substituting $\varepsilon_{sm} = \varepsilon_{ir} = 1$, $A = 0$, and $\chi = 4$. Substitution yields the equivalent blackbody diameter

$$d_{BB} = 6\,\lambda\,\Delta\,S_\nu^{1/2}\,R^{1/4} \quad (4)$$

defined as the diameter of the blackbody, in kilometers, required to produce the same flux density as the comet when placed at the location of the nucleus. In Eq. (4), R and Δ are expressed in astronomical units S_ν is in millijanskys and λ is in millimeters. Values of d_{BB} are given in column 5 of Table IV.

Table IV shows that the detected comets have d_{BB} in the range from 7 km (IRAS–Araki–Alcock) to ~40 km (P/Brorsen–Metcalf and P/Halley). The effective diameter of the nucleus of IRAS–Araki–Alcock estimated from observations at other wavelengths is $6 \le d \le 12$ km (Goldstein *et al.* 1984). Thus, the millimeter continuum of this comet is consistent with a detection of thermal radiation from the nucleus (c.f. Altenhoff *et al.* 1983). The blackbody diameter of Okazaki–Levy–Rudenko ($d_{BB} = 12 \pm 1$ km; Table IV) is also consistent with the likely size of the nucleus, so that we must conclude that in this comet a significant but uncertain fraction of the detected radiation may emanate from the nucleus. However, in the other detected comets, d_{BB} is significantly larger than the ~5–10 km expected size of the nucleus (e.g. P/Halley; see also Jewitt 1991). Therefore, the submillimeter and millimeter emission is unlikely to be thermal radiation solely from the nucleus, as was already noted in the case of P/Halley by Altenhoff *et al.* (1989). Instead, this radiation must be attributed, in part, to solid particles in the coma.

4.3. Coma

What mass of particulate coma is needed to account for the observed submillimeter emissions? A detailed calculation of the mass was described in JL90; here we adopt a simplified but nevertheless valid approach. The mass, M (kg), can be estimated from

$$M = \frac{S_\nu\,\Delta^2}{B_\nu(T)\,\kappa(\lambda)}, \quad (5)$$

where $B_\nu(T)$ (W m^{-2} Hz^{-1} sr^{-1}) is the Planck function at temperature T (K), and $\kappa(\lambda)$ (m^2 kg^{-1}) is the opacity. Strictly, temperature T should be computed for each grain size from the equation of radiative equilibrium, while taking into account the wavelength dependence of the absorption cross section. This was done explicitly in JL90, with the result that "superheating" of grains due to emissivity variations had a negligible effect on the emitted spectrum (see Fig. 2 of that paper). For our present purposes, it is sufficient to take the temperature of a spherical, isothermal blackbody $T \sim 278/R^{1/2}$ as a first estimate of the grain temperature. At the temperatures of the comets considered here, $B_\nu(T)$ falls well within the Rayleigh–Jeans regime and is thus relatively insensitive to uncertainties in the temperature.

The principal uncertainties in the estimation of masses using Eq. (5) result from the unknown opacity of cometary

TABLE IV
Summary of Observations

Comet[a]	R [AU][b]	λ [mm][c]	S_ν [mJy][d]	d_{bb} [km][e]	M_1 [kg][f]	M_2 [kg][g]	Reference[h]
P/Brorsen-Metcalf	0.48	0.8	90 ± 18	41 ± 4	$3.6 \pm 0.7 \times 10^9$	$1.1 \pm 0.2 \times 10^8$	This Work
Austin 1989c$_1$	0.57	0.8	≤ 38	≤ 16.6	$\leq 6 \times 10^8$	$\leq 1.8 \times 10^7$	This Work
O-L-R	0.67	0.8	21 ± 4	12 ± 1	$3.2 \pm 0.6 \times 10^8$	$9.6 \pm 2 \times 10^6$	This Work
Austin 1989c$_1$	0.75	1.2	12 ± 2	34 ± 3	$3.7 \pm 0.6 \times 10^9$	$1.1 \pm 0.2 \times 10^8$	Altenhoff *et al.* (1990)
IRAS–Araki–Alcock	1.00	13	9.0 ± 0.7	7.3 ± 0.3	$1.9 \pm 0.1 \times 10^9$	$5.6 \pm 0.4 \times 10^7$	Altenhoff *et al.* (1983)
P/Halley	1.13	1.2	52 ± 5	32 ± 2	$3.2 \pm 0.3 \times 10^9$	$9.7 \pm 1 \times 10^7$	Altenhoff *et al.* (1989)
P/Faye	1.59	1.1	≤ 8	≤ 13.4	$\leq 5.7 \times 10^8$	$\leq 1.7 \times 10^7$	This Work
P/Halley	1.60	1.3	52 ± 15	40 ± 6	$5.3 \pm 1.0 \times 10^9$	$1.6 \pm 0.5 \times 10^8$	Altenhoff *et al.* (1986)
P/Halley	1.60	3.5	5.9 ± 1.4	36 ± 4	$1.2 \pm 0.3 \times 10^{10}$	$3.7 \pm 0.9 \times 10^8$	Altenhoff *et al.* (1986)
Levy 1990c	1.67	1.1	≤ 14	≤ 24.8	$\leq 1.9 \times 10^9$	$\leq 5.7 \times 10^7$	This Work

[a] Comet name
[b] Helocentric distance [AU]
[c] Wavelength [mm]
[d] Flux density [mJy]
[e] Equivalent blackbody diameter [km]
[f] Mass using Mie opacity [kg]
[g] Mass using fractal opacity [kg]
[h] Reference.

dust at submillimeter wavelengths, $\kappa(\lambda)$. The opacity is a function of the wavelength of observation, the grain size and its distribution, the grain composition, and even of the shape of the grains (van de Hulst 1957, Bohren and Huffman 1983, Berry and Percival 1986). To illustrate these uncertainties, we present masses based on two extreme values of the submillimeter opacity.

First, we consider a coma of grains in which the differential size distribution is

$$n(a)da = \Gamma\, a^{-q}\, da, \qquad (6)$$

where a (m) is the grain radius and Γ and q are constants. The size distribution is taken to extend from a minimum radius, $a-$, to a maximum radius, $a+$. The effective opacity at wavelength λ is then

$$\kappa_1(\lambda) = \frac{\int_{a-}^{a+} Q_a(\lambda)\, \pi a^2\, n(a)\, da}{\int_{a-}^{a+} (4\pi/3)\, \rho\, a^3\, n(a)\, da}, \qquad (7)$$

where $Q_a(\lambda)$ is the (dimensionless) absorption efficiency of the grains. We calculated the $Q_a(\lambda)$ for spherical, homogeneous particles of three different compositions using the Mie theory (van de Hulst 1957, Bohren and Huffman 1983). As we will soon note, it is likely that the grains in comets are *not* homogeneous spheres. Nevertheless, Mie theory calculations are helpful in showing the sensitivity of the opacity to variations in the grain composition and size distribution. Calculations were made using the wavelength-dependent complex refractive indices of silicate (Draine 1985), glassy carbon (Edoh 1983), and Tholin (Khare *et al.* 1984). Again, these materials were chosen as broadly representative of the types of matter thought to be present in comet dust. Equations (6) and (7) were then solved using size distribution indices $q = 3$ and $q = 4$, as suggested by the size distribution of the grains in P/Halley (McDonnell *et al.* 1987). Sample results are listed in Table V.

TABLE V
Sample Opacities at $\lambda = 1$ mm

Model Number	$a-$ [mm]	$a+$ [mm]	Size index q	Material	κ_1 [m^2 kg^{-1}]
1	10^{-5}	1	3	Silicate	0.68
2	10^{-5}	10	3	Silicate	0.13
3	10^{-5}	100	3	Silicate	0.02
4	10^{-5}	1	3	Carbon	0.89
5	10^{-5}	10	3	Carbon	0.13
6	10^{-5}	100	3	Carbon	0.02
7	10^{-5}	1	3	Tholin	0.79
8	10^{-5}	10	3	Tholin	0.24
9	10^{-5}	100	3	Tholin	0.04
10	10^{-5}	1	4	Silicate	0.30
11	10^{-5}	10	4	Silicate	0.27
12	10^{-5}	100	4	Silicate	0.24
13	10^{-5}	1	4	Carbon	1.18
14	10^{-5}	10	4	Carbon	1.01
15	10^{-5}	100	4	Carbon	0.85
16	10^{-5}	1	4	Tholin	0.33
17	10^{-5}	10	4	Tholin	0.32
18	10^{-5}	100	4	Tholin	0.28

The calculated opacities were found to be insensitive to the lower size limit, $a-$, provided $a- \ll \lambda$ and $a- \ll a+$. The physical explanation is that the small grains, although numerous, are inefficient radiators at submillimeter wavelengths and thus contribute weakly to the opacity. For definiteness, the sample results in Table V all have $a- = 10^{-5}$ mm. The opacities are more sensitive to the upper size limit, $a+$. As discussed in Section 1, the existence of millimeter-sized grains in active, near-Sun comets is known with confidence (e.g., Eaton *et al.* 1984, McDonnell *et al.* 1987). Gas drag is sufficient to eject grains 1 to 2 orders of magnitude larger still (Whipple 1950). Accordingly, in Table V we summarize calculations made using $a+ = 1$, 10, and 100 mm. The table shows that the effective opacity decreases as $a+$ increases in this radius range, apparently because the larger particles become individually optically thick and so contribute to the mass faster than they contribute to the radiating cross section. This is especially true of the $q = 3$ distribution, in which the total grain mass is determined by the largest particles.

The effective opacity varies by more than an order of magnitude among the 18 sample models in Table V. From consideration of these and other models based on Eq. (7), we adopt

$$\kappa_1(\lambda)\,(\mathrm{m^2\,kg^{-1}}) = \frac{0.3}{\lambda\,(\mathrm{mm})} \tag{8}$$

as a representative opacity for Mie spheres in Halley-like size distributions. The uncertainty in Eq. (8) is best judged by inspection of Table V. This is also the value adopted by Beckwith *et al.* (1990) in their submillimeter study of dusty pre-main-sequence stars. We note for comparison that Hildebrand (1983) proposed κ (1 mm) ~ 0.06 m^2 kg^{-1} (with an estimated uncertainty of a factor of 4) for dust in the interstellar medium. Draine (1990) has compared various estimates of the long wavelength opacity of interstellar grains. Note that real differences may exist among the opacities of grains in different environments. The very large grains included in our calculation of κ_1, for instance, would probably be absent from dust in the interstellar medium.

Dust masses computed using Eq. (8) are denoted M_1 and are listed in column 6 of Table IV. There it may be seen that $M_1 \sim 10^8$–10^9 kg for each of the detected comets (P/Brorsen–Metcalf, Austin, O-L-R, and P/Halley). For comparison, the total mass released from P/Halley during the entire 1986 apparition is estimated at 5×10^{11} kg (Whipple 1987). Evidently, large dust masses are implied by the opacity formula in Eq. (8).

The grains in comets are likely to be porous aggregates of smaller grains, for which submillimeter opacities larger than κ_1 are anticipated (Wright 1987, 1989, Hage and Greenberg 1990). High porosity is a natural consequence of particle growth by aglomeration (Brooks 1990, Meakin and Donn 1988, Donn 1990). Some extraterrestrial stratospheric dust particles, thought to be of cometary origin, are highly porous (Brownlee *et al.* 1980). Impact counters on the Giotto spacecraft detected clustered impacts produced by the fragmentation of weakly bound grains while in flight (Simpson *et al.* 1987). Several authors have reported very large opacities for conducting fractal aggregates (e.g., Berry and Percival 1986, Wright 1987). From Fig. 6 of Wright (1987) we estimate a fractal grain opacity

$$\kappa_2(\lambda)\,(\mathrm{m^2\,kg^{-1}}) = \frac{10}{\lambda\,(\mathrm{mm})}\,. \tag{9}$$

Masses computed using Eq. (9) are denoted M_2 and are listed in column 7 of Table IV. There it may be seen that $M_2 \sim 10^7$–10^8 kg. Thus, the very large opacities of fractal grains greatly reduce the mass of dust needed to supply a given flux density.

How are the derived dust masses M_1 and M_2 to be interpreted? Consider an active comet observed at $R = \Delta = 1$ AU. Suppose that the nucleus loses dust at the rate dM_d/dt (kg sec^{-1}), and that the dust has terminal velocity v (m sec^{-1}). The time of residence of the dust inside the photometry diaphragm is $\tau \sim \phi\,\Delta/(2\,v)$, where ϕ (rad) is the diaphragm diameter. Therefore, the mass of dust projected within the diaphragm is $M_d \sim dM_d/dt\;\phi\,\Delta/(2\,v)$.

For definiteness, we consider the case of Comet P/Halley. The mass loss rate in dust at $R = 1$ AU was $dM_d/dt \sim 10^4$ kg sec^{-1} (Tokunaga *et al.* 1986, Gehrz and Ney 1992). We take the outflow speed of small grains to be comparable to the speed of sound in the coma gas, $v \sim 500$ m sec^{-1}. The angular diameter of the beam used to observe the comet was $\phi = 11$ arcsec $= 5.4 \times 10^{-5}$ rad (Altenhoff *et al.* 1989). Substitution gives the dust mass within the beam $M_d \sim 5 \times 10^7$ kg. For comparison, the dust mass in P/Halley estimated using opacity κ_2 is $M_2 \sim$ (1 to 4) $\times 10^8$ kg (see Table IV). The evident agreement within a factor 2 to 8 must be partly fortuitous—neither dM_d/dt nor v is known with confidence at the time of the millimeter measurement. But the observation that $M_d \sim M_2$ shows that fractal particles can provide a plausible explanation of the cometary submillimeter continuum without requiring huge masses of dust in the coma.

Alternate interpretations of the radio continuum emission have been proposed in terms of centimeter-sized ice grains (Gibson and Hobbs 1981) and meter-sized boulders (Walmsley 1985). As noted earlier (Section 4.3), the submillimeter cross section per unit mass decreases as the particles grow large compared to a wavelength. Therefore, these interpretations require proportionately larger masses of material to provide a given submillimeter signal. The optically thick ice grain halo model is essentially ruled out by numerous direct observations of cometary nuclei in recent years (c.f. Jewitt 1991). Moreover, any process capable of lifting centimeter- and meter-sized objects from the cometary nucleus would simultaneously eject far larger numbers of small particles. Thus, it seems more natural to interpret the submillimeter emission in terms of broad size distributions of particles, as in the present work, rather than in terms of populations of ultra-large grains or boulders.

5. FUTURE MEASUREMENTS

Future observations may allow us to distinguish between submillimeter continuum emission from the porous particles discussed in Section 4 and continuum emitted by millimeter-sized compact particles, as discussed in a previous work (JL90). Such discrimination would be based on the spatial distribution of the submillimeter continuum. The porous particles discussed here possess a large cross section per unit mass so that they will be well coupled to the gas flow from the nucleus (Meakin and Donn 1988). These particles will be ejected from the nucleus at a speed comparable to the speed of sound in the coma and will populate a near-spherical volume around the nucleus analogous to the well-known optical dust coma. By contrast, large compact particles have a small cross section per unit mass, will be ejected from the nucleus at low speeds, and will spread preferentially in the orbit plane in the same way that the IRAS particles are confined (Eaton *et al.* 1984). A submillimeter image of a comet would reveal a nearly spherical coma in the former case, but a sheet-like, highly elongated coma in the latter. Such an image would also clearly delineate emission from the nucleus, should it be detectable.

A submillimeter map of Comet Austin has been presented by Chakaveh *et al.* (1990). This map shows nearly circular isophotes that are consistent with high velocity particles distributed in a near-spherical coma. It thus lends support to the present interpretation of the submillimeter continuum as thermal emission from porous particles. Unfortunately, the scale of the map (50 × 50 arcsec) is only ~2.5 times larger than the diffraction resolution of the JCMT (18 arcsec at 1.1 mm), so that it is difficult to ascertain the true morphology of the submillimeter coma.

We expect that compelling imaging observations will be provided by the next-generation submillimeter-array bolometer, SCUBA (Gear and Cunningham 1990). SCUBA is to be commissioned at the JCMT in mid-1993. The primary advantages of SCUBA over UKT14 for cometary studies are

- SCUBA consists of two arrays (37 pixels at 850 μm and 91 pixels at 450 μm) illuminated simultaneously via a dichroic mirror. The field of view is approximately 2.5 arcmin in each array. The use of an array will permit direct imaging of resolved cometary sources and will allow increased observing efficiency by providing simultaneous sky monitoring on point sources.
- Each pixel in SCUBA is about 10 times more sensitive than the UKT14 bolometer, as a result of the very low operating temperature (0.1 K). The enhanced sensitivity will allow a greater detection rate among comets.
- Additional "photometric pixels" provide wavelength coverage up to 2 mm, with filters typically having $\lambda/\Delta\lambda \sim$ 4 to 5.

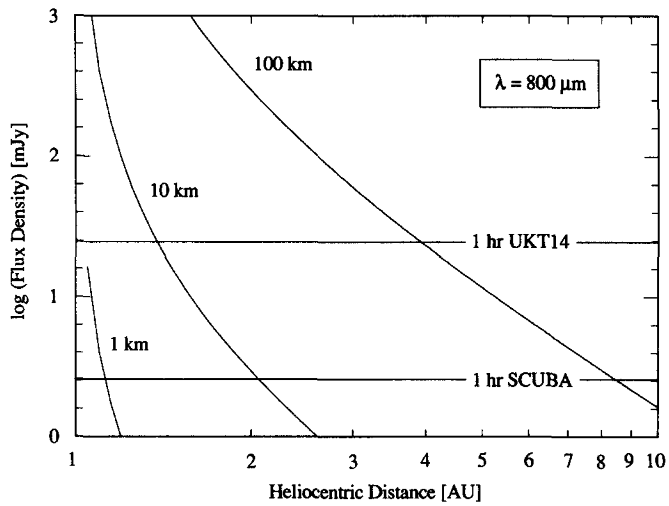

FIG. 1. Flux density F_ν [mJy] versus heliocentric distance R [AU] computed from Eq. (3). The labels give the diameters of three spherical, isothermal blackbodies observed at opposition. The 3σ, 1-hr sensitivities of UKT14 and the SCUBA bolometer array are marked.

To illustrate the advantages expected from SCUBA for cometary studies, we used Eq. (3) to compute opposition flux densities (i.e., $\Delta = R - 1$, for $R > 1$) for three spherical, isothermal blackbodies as a function of heliocentric distance and object diameter. The results are plotted in Fig. 1. The 3σ sensitivities obtained with UKT14 and SCUBA after 1 hr of on-source integration under good atmospheric conditions are marked in the figure (note that 1 hr of on-source integration with UKT14 corresponds to about 3 hr of observing time, as discussed in Section 2. Figure 1 shows the dramatic improvement in sensitivity conveyed by SCUBA. With this instrument, the nuclei of short period comets should be routinely detectable out to distances of $R \sim 2$ AU, opening a new window for the study of these enigmatic bodies.

CONCLUSIONS

The present observations serve to demonstrate that a significant fraction of near-Earth comets emit submillimeter radiation at the 10- to 100-mJy level and so are within reach of existing submillimeter telescopes. Specifically,

1. Five comets (two periodic and three dynamically new) have been observed at 0.8-mm and 1.1-mm wavelengths with the JCMT, using the single-channel bolometer UKT14. One periodic (P/Brorsen–Metcalf) and one dynamically new comet (Okazaki–Levy–Rudenko) were detected. Independent millimeter wavelength detections of P/Halley, IRAS–Araki–Alcock, and Austin 1989c_1 by Altenhoff *et al.* (1983, 1986, 1989) are also discussed.

2. The long wavelength continuum is tentatively attributed to thermal emission from porous, possibly fractal particles in the coma. The inferred coma particle masses are $\sim 10^7$ to 10^8 kg, when computed using the fractal grain opacities of Wright (1987). Emission from Mie spheres can also explain the radiocontinuum. However, spheres are poorer emitters than fractal aggregates, and larger masses of dust (10^8 to 10^9 kg) would then be required.

3. The continuum flux densities are larger than can be produced by free–free radiation from cometary plasma.

4. A significant fraction of the emission from Comets IRAS–Araki–Alcock and Okazaki–Levy–Rudenko may emanate from the nucleus.

5. Important constraints may be placed on the nature of the submillimeter emitters using continuum mapping observations. Small porous particles should be ejected from the nucleus at high speed and will occupy a spherical coma resembling the optical dust coma. Compact millimeter-sized particles should be confined to the cometary orbital plane, resulting in a coma that is highly elongated along the direction of the projected orbit. Diagnostic submillimeter maps await the completion of the SCUBA bolometer array.

ACKNOWLEDGMENTS

We thank the JCMT operators and support scientists for their assistance. We are very grateful to Graeme Watt for scheduling our target-of-opportunity observations of Comet Okazaki–Levy–Rudenko in 1989 and to Jim Annis for help with the observations of P/Faye. We thank W. Altenhoff for his comments on a draft of this paper. This work was supported by an NSF grant for the submillimeter astronomy of comets to David Jewitt and by a Harvard–Smithsonian Postdoctoral fellowship to Jane Luu.

REFERENCES

Altenhoff, W. J., W. Batrla, W. K. Huchtmeier, J. Schmidt, P. Stumpff, and C. M. Walmsley 1983. Radio observations of Comet 1983d. *Astron. Astrophys.* **125,** L19–L22.

Altenhoff, W. J., W. K. Huchtmeier, J. Schmidt, J. B. Schraml, P. Stumpff, and C. Thum 1986. Radio continuum observations of Comet Halley. *Astron. Astrophys.* **164,** 227–230.

Altenhoff, W. J., W. K. Huchtmeier, E. Kreysa, J. Schmidt, J. B. Schraml, and C. Thum 1989. Radio continuum observations of Comet P/Halley at 250 GHz. *Astron. Astrophys.* **222,** 323–328.

Altenhoff, W. J., E. Kreysa, J. Schmidt, and J. B. Schraml 1990. IAUC 4993, April 13.

Balsiger, H., K. Altwegg, F. Bühler, J. Geiss, A. G. Ghielmetti, B. E. Goldstein, R. Goldstein, W. T. Huntress, W.-H. Ip, A. J. Lazarus, A. Meier, M. Neugebauer, U. Rettenmund, H. Rosenbauer, R. Schwenn, R. D. Sharp, E. G. Shelley, E. Ungstrup, and D. T. Young 1986. Ion compositions and dynamics at Comet Halley. *Nature* **321,** 330–334.

Beckwith, S. V. W., A. I. Sargent, R. S. Chini, and R. Güsten 1990. A survey for circumstellar disks around young stellar objects. *Astron. J.* **99,** 924–945.

Berry, M. V., and I. C. Percival 1986. Optics of fractal clusters such as smoke. *Opt. Acta* **33,** 577–591.

Bohren, C. F., and D. R. Huffman 1983. Absorption and scattering of light by small particles. Wiley, New York.

Brooks, A. 1990. Aggregation of grains in the protosolar nebula. In *Asteroids, Comets, Meteors III* (C. I. Lagerkvist, H. Rickman, B. A. Lindblad, and M. Lindgren, Eds.), pp. 25–28. Uppsala University Press, Uppsala.

Brownlee, D. E., L. Pilachowski, E. Olszewski, and P. W. Hodge 1980. In *Solid Particles in the Solar System* (I. Halliday and B. A. McIntosh, Eds.), pp. 333–342. Reidel, Boston.

Campbell, D. B., J. K. Harmon, and I. I. Shapiro 1989. Radar observations of Comet P/Halley. *Astrophys. J.* **338,** 1094.

Chakaveh, S., W. Dent, C. D. Kaminski, and E. K. Jessberger 1990. In *Proc. 24th ESLAB Symposium on the Formation of Stars and Planets,* (B. Battrick, Ed.), pp 209–211. ESA SP-315, Noordwijk.

Crovisier, J., and F. P. Schloerb 1991. In *Comets in the Post-Halley Era,* (R. L. Newburn, M. Neugebauer. and J. Rahe, Eds.), Vol. 1, pp. 149–173. Kluwer Academic, Dordrecht.

Davies, J. K., S. F. Green, B. C. Stewart, A. J. Meadows, and H. H. Aumann 1984. The IRAS fast-moving object search. *Nature* **309,** 315–319.

Donn, B. D. 1990. The formation and structure of fluffy cometary nuclei from random accumulation of grains. *Astron. Astrophys.* **235,** 441–446.

Draine, B. T. 1985. Tabulated optical properties of graphite and silicate grains. *Astrophys. J. Suppl. Ser.* **57,** 585–594.

Draine, B. T. 1990. In *The Interstellar Medium in Galaxies* (H. A. Thronson and J. M. Shull, Eds.), pp. 483–492. Kluwer, Dordrecht.

Duncan, W. D., E. I. Robson, P. A. R. Ade, M. J. Griffin, and G. Sandell 1990. A millimetre/submillimetre common user photometer for the James Clerk Maxwell Telescope. *Mon. Not. R. Astron. Soc.* **243,** 126–132.

Eaton, N., J. K. Davies, and S. F. Green 1984. The anomalous dust tail of Comet P/Tempel 2. *Mon. Not. R. Astron. Soc.* **211,** 15P–19P.

Edoh, O. 1983. Ph.D. thesis, University of Arizona.

Gear, W., and C. Cunningham 1990. In *Proc. 29th Liege International Astrophysical Colloquium, Liege, Belgium, 3–5 July 1990.* ESA SP-314, pp. 353–358.

Gehrz, R. D., and E. P. Ney 1992. 0.7- to 23-μm photometric observations of P/Halley 1986 III and six recent bright comets. *Icarus,* in press.

Gibson, D. M., and R. W. Hobbs 1981. On the microwave emission from comets. *Astrophys. J.* **248,** 863–866.

Goldstein, R. M., R. F. Jurgens, and Z. Sekanina 1984. A radar study of Comet IRAS–Araki–Alcock 1983d. *Astron J.* **89,** 1745–1754.

Hage, J. I., and Greenberg, J. M. 1990. A model for the optical properties of porous grains. *Astrophys. J.* **361,** 251–259.

Harmon, J. K., D. B. Campbell, A. A. Hine, I. I. Shapiro, and B. G. Marsden 1989. Radar observations of comet IRAS–Araki–Alcock 1983d. *Astrophys. J.* **338,** 1071–1093.

Hildebrand, R. H. 1983. The determination of cloud masses and dust characteristics from submillimetre thermal emission. *Q. J. R. Astron. Soc.* **24,** 267–282.

HOBBS, R. W., S. P. MARAN, J. C. BRANDT, W. J. WEBSTER, AND K. S. KRISHNA SWAMY 1975. Microwave continuum radiation from Comet Kohoutek 1973f: Emission from the icy-grain Halo? *Astrophys. J.* **201,** 749–755.

HOBBS, R. W., J. C. BRANDT, AND S. P. MARAN 1977. Microwave continuum radiation from Comet West 1975n. *Astrophys. J.* **218,** 573–578.

JEWITT, D. C. 1991. Cometary photometry. In *Comets In The Post—Halley Era,* (R. Newburn, M. Neugebauer, and J. Rahe, Eds.), pp. 19–65. Kluwer Academic, Dordrecht.

JEWITT, D. C., AND J. X. LUU 1989. IAU Circular 4852 (September 13).

JEWITT, D. C., AND J. X. LUU 1990. The submillimeter radio continuum of Comet P/Brorsen–Metcalf. *Astrophys. J.* **365,** 738–747.

JEWITT, D. C., AND J. X. LUU 1992. Submillimeter continuum observations of 2060 Chiron. *Astron. J.* **104,** 398–404.

KHARE, B. N., C. SAGAN, E. T. ARAKAWA, F. SUITS, T. A. CALLCOTT, AND M. W. WILLIAMS 1984. Optical constants of organic tholins produced in a simulated titanian atmosphere. *Icarus* **60,** 127–137.

MCDONNELL, J. A. M., *et al.* 1987. The dust distribution within the inner coma of Comet P/Halley 1982i: Encounter by Giotto's impact detectors. *Astron. Astrophys.* **187,** 719–741.

MEAKIN, P., AND B. DONN 1988. Aerodynamic properties of fractal grains: Implications for the primordial solar nebula. *Astrophys. J.* **329,** L39–L41.

REINHARD, R. 1987. In *Exploration of Halley's Comet* (M. Grewing, F. Praderie, and R. Reinhard, Eds.), pp 949–958. Springer-Verlag, Berlin.

SANDELL, G. 1992. In preparation.

SCHWENN, R., W.-H. IP, H. ROSENBAUER, H. BALSIGER, F. BÜHLER, R. GOLDSTEIN, A. MEIER, AND E. G. SHELLEY 1987. Ion temperature and flow profiles in Comet P/Halley's close environment. *Astron. Astrophys.* **187,** 160–162.

SIMPSON, J. A., D. RABINOWITZ, A. J. TUZZOLINO, L. V. KSANFOMALITY, AND R. Z. SAGDEEV 1987. The dust coma of comet P/Halley: Measurements on the Vega-1 and Vega-2 spacecraft. *Astron. Astrophys.* **187,** 742–752.

SNYDER, L. E. 1982. A review of radio observations of comets. *Icarus* **51,** 1–24.

SPITZER, L. 1978. *Physical Processes in the Interstellar Medium,* pp. 57–59. Wiley, New York.

SYKES, M., D. M. HUNTEN, AND F. J. LOW 1986. The discovery of dust trails in the orbits of periodic comets. *Science* **232,** 1115–1117.

TOKUNAGA, A. T., W. F. GOLISCH, D. M. GRIEP, C. KAMINSKI, AND M. S. HANNER, 1986. The NASA Infrared Telescope Facility Comet Halley monitoring program. I. Preperihelion results. *Astron. J.* **92,** 1183–1190.

VAN DE HULST, H. C. 1957. *Light Scattering by Small Particles.* Wiley, New York.

WALMSLEY, C. M. 1985. The interpretation of the radio continuum emission from Comet IRAS–Araki–Alcock (1983d). *Astron. Astrophys.* **142,** 437–440.

WHIPPLE, F. 1950. A comet model. I. The acceleration of Comet Encke. *Astrophys. J.* **111,** 375–394.

WHIPPLE, F. 1987. The cometary nucleus: Current concepts. *Astron. Astrophys.* **187,** 852–858.

WILLIAMS, I. P. 1990. In *Asteroids, Comets, Meteors III,* (C. I. Lagerkvist, H. Rickman, B. A. Lindblad, and M. Lindgren, Eds.), pp. 585–594. Uppsala University Press, Uppsala.

WRIGHT, E. L. 1987. Long wavelength absorption by fractal dust grains. *Astrophys. J.* **320,** 818–824.

WRIGHT, E. L. 1989. Fractal dust grains around R coronae borealis stars. *Astrophys. J.* **346,** L89–L91.